Microchimica Acta (2021) 188:252
https://doi.org/10.1007/s00604-021-04918-7

ORIGINAL PAPER

Monose-modified organic electrochemical transistors for cell surface glycan analysis via competitive recognition to enzyme-labeled lectin

Lizhen Chen[1] · Jie Wu[1] · Feng Yan[2] · Huangxian Ju[1]

Received: 21 March 2021 / Accepted: 27 June 2021

Abstract

A competitive strategy for glycan determination on cell surface with organic electrochemical transistors (OECTs) has been developed. The carboxylic multi-wall carbon nanotubes were firstly immobilized on the gate interface to cross-link the specific monose with adipic dihydrazide as the linker, which could then competitively recognize horseradish peroxidase (HRP)–labeled lectin with the target monose on the cell surface. The HRP captured on the gate interface through the affinity of lectin to monose finally catalyzed the reduction of hydrogen peroxide to produce the output current signal for detection of cell surface monose under the optimal gate voltage of 0.9 V. Using mannose and galactose groups as the target models, HRP-labeled concanavalin A and peanut agglutinin were used to competitively recognize these groups on both cell surface and gate interface, respectively. The amounts of mannose and galactose on HeLa cells were measured to be 3.41×10^8 and 2.92×10^8 molecules per cell, respectively. The changes of the mannose and galactose expressions upon external stimulation were also observed with the proposed biosensors, which showed consistent results with flow cytometric analysis, indicating that the OECT-based biosensor is suitable for analysis of different glycan expressions on cell surface.

Keywords Organic electrochemical transistor · Competitive recognition · In situ glycan determination · Lectin · Mannose · Galactose

Introduction

Glycans, which decorate on the mammalian cell surface through the glycosylation of proteins, play important roles in intercellular processes [1–4]. Various glycan binding sites on proteins lead to their complex structures on cell surface, and abnormal expression of glycans on cell surface is associated with the certain disease status [5–7]; thus, the quantitative analysis of glycan on cell surface may provide valuable information for disease diagnoses, and the cell surface glycan analysis has been quickly developed with different detection technologies such as Raman spectrometry [8], mass spectrometry [9, 10], fluorescence imaging [11], and electrochemical methods [12–14].

As a detection platform, the organic electrochemical transistors (OECTs) are consisted of gate, drain, and source electrodes with an organic semiconductor film between drain and source electrodes [15, 16]. This detection technology possesses high sensitivity owing to the inherent amplification function of transistors [17] and stable performances in liquid electrolytes under low working voltage [18]. It can be used for detecting both electroactive [19–21] and electro-inactive molecules [22–24] or biomacromolecules [25, 26] through the electrostatic interactions or affinity bindings between targets and functionalized channel or gate interface. To extend the application of OECTs in cytosensing and glycan analysis, our previous work used concanavalin A to modify the gate electrode for capture of target cells, and then introduction of nanoprobe functionalized with aptamer and horseradish peroxidase (HRP) onto electrode surface through the recognition of aptamer with specific cell surface protein, which produced detectable signal via HRP-catalyzed reduction reaction of hydrogen peroxide (H_2O_2) on gate interface [27]. Obviously, this method was rather complex and could not quantitatively detect the cell surface glycan expression. Thus, we designed a facile sensing strategy for quantitation of glycans on cell surface through covalently binding target cells on

✉ Huangxian Ju
hxju@nju.edu.cn

[1] State Key Laboratory of Analytical Chemistry for Life Science, School of Chemistry and Chemical Engineering, Nanjing University, Nanjing 210023, China

[2] Department of Physics, The Hong Kong Polytechnic University, Hong Kong, Hong Kong

Published online: 13 July 2021

mercaptopropionic acid–modified gate electrode for the recognition of HRP-labeled lectin (HRP-lectin) and simulating the cells with glycan-modified microspheres for obtaining the calibration curves [28]. These works indicated the practical application of the OECT-based biosensors in cell surface glycan expression analysis.

To simplify the quantitative detection of cell surface glycans and avoid the relative complex synthesis of modified microspheres [28], this work designed monose-modified gate electrodes for competitive capture of HRP-labeled lectins with cell surface glycans, which directly produced the detectable signal in the presence of H_2O_2 and greatly accelerated the quantitation procedure of cell surface glycans. The monose functionalized gate electrode could be conveniently prepared by binding monose to carboxylic multi-wall carbon nanotubes (CNTs) immobilized gate interface with adipic dihydrazide (ADH) as the linker. Thus, the corresponding HRP-lectin could be used to competitively recognize the monose bound on gate interface and target glycan on cell surface. The presence of cell surface glycan decreased the amount of HRP-lectin bound to electrode surface and thus the output signal. Interestingly, the calibration curves could be easily obtained with the monose standard solutions. As a proof-of-concept, the designed biosensing strategy realized the analysis of mannose and galactose on HeLa cells. This work provided a new feasible strategy for the quantitative analysis of cell surface glycan expression.

Experimental section

Materials and apparatus

CNTs were purchased from XFNANO Materials Tech Co., Ltd. (Nanjing, China). PEDOT:PSS (Clevios™, PH 1000) was provided by Heraeus (Germany). The other materials and apparatus are described in the Electronic Supplementary Material (ESM†).

Modification of gate electrode

The OECTs were prepared according to the previous work (ESM†) [28]. The commercial CNTs were firstly dispersed under ultrasonication, and then 10 μL of CNTs dispersion wasdropped on gate electrode to form a thin layer at room temperature. Afterward, 10 μL of the mixture of 3 mg/mL EDC and 2 mg/mL ADH dissolved in DMSO was dropped on the CNT-modified gate electrode and incubated at room temperature for 6 h. Next, 10 μL of mannose or galactose solution was dropped on the gate interface for another 12 h to covalently immobilize mannose or galactose on the gate interface. Finally, 10 μL of 1% wt BSA was dropped on the gate interface to block the active surface at room temperature for 30 min. After rinsing the modified gate interface with PBS, the OECT-based biosensor was obtained.

Cell surface glycan detection

For glycan analysis on cell surface, 10 μL of HRP-lectin mixed with monose or cells was dropped on the OECT-based biosensor (functionalized gate electrode) for competitively binding of lectin to specific monose at 4 °C for 1 h. After rinsing the modified gate interface with PBS, the measurement of the drain-source channel current was performed at the gate voltage of 0.9 V and the drain-source voltage of 0.05 V by immersing the OECT-based biosensor in pH 7.4 PBS containing 100 μM H_2O_2.

Results and discussion

Biosensing strategy for cell surface glycans analysis

The CNTs coated on the gate electrode were firstly activated with EDC to covalently binding with ADH, and the mannose or galactose was then introduced to the gate surface with ADH as the linker (Fig. 1). The HRP-lectin was captured on the gate interface through the specific recognition of lectin to mannose or galactose. Reasonably, the amount of HRP-lectin captured on the gate interface was related to the immobilized glycan. When the mixture of HRP-lectin and cells or corresponding monose was incubated on the gate interface, some HRP-lectin molecules were captured by the corresponding glycan on cell surface or bound with the monose in solution, which led to the decrease of HRP-lectin captured on the gate interface. Thus, the output signal resulted from the HRP-catalyzed reduction of H_2O_2 on gate/electrolyte interface decreased, leading to a simple biosensing strategy for glycan analysis on cell surface. Furthermore, the calibration curves for quantitative detection of cell surface glycans could be obtained with the monose standard solutions.

Characterization of gate electrodes

The fresh OECT was tested in PBS to obtain the typical transfer curve. The drain-source current showed the change of more than one order of magnitude under the gate voltage ranging from 0 to 1.2 V (Fig. 2a). The transconductance (g_m), which is defined as the differentiation of the channel current against gate voltage, showed the maximum value of 0.85 mS at the gate voltage of 0.9 V. This work measured the steady channel currents before (I_0) and after (I) addition of 100 μM H_2O_2 within 500 s to obtain the detection signal by fixing the drain-source voltage at 0.05 V. Here the detection signal is defined as $\Delta I/I_0$, and ΔI is the channel current change upon addition of H_2O_2. The optimized gate voltage for the analysis of cell surface glycans also appeared at 0.9 V (Fig. S1).

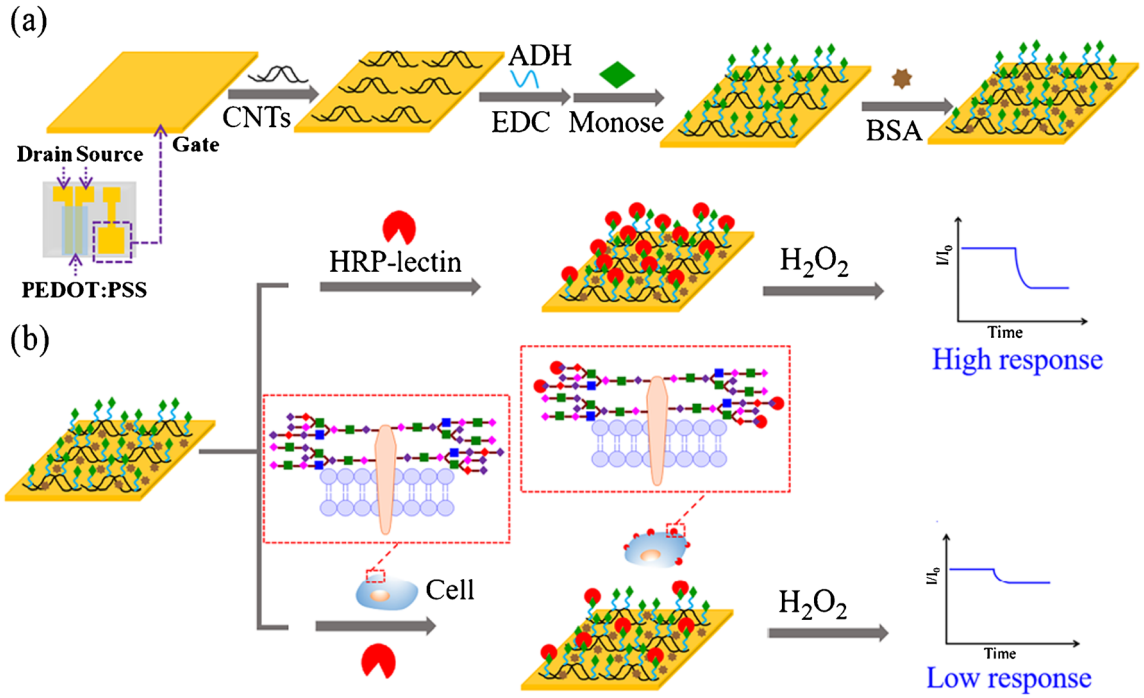

Fig. 1 Schematic illustration of (a) of OECT modification and (b) OECT-based biosensing for glycan analysis on cell surface

The Zeta potentials were detected to examine the charge changes of CNTs after binding ADH and linking glycans. After ADH was bound to CNTs, the Zeta potential became a positive value due to the presence of -NH_2 group of ADH. After mannose was linked to ADH functionalized CNTs, the Zeta potential decreased owing to the amino-based ligation (Fig. S2a).

The EIS measurements were used to characterize the modification and recognition process on gate interface (Fig. 2b). CNT-modified gate electrode showed a relatively low electron-transfer resistance around 500 Ω (curve a) and a well-dispersed structure of CNTs film with the form of small bundles or single tubes (Fig. S2b). The resistance greatly increased to ~1200 Ω after the mannose was linked to CNTs via ADH (curve b). The electron-transfer resistance further increased to 1800 Ω after BSA was adsorbed on the electrode interface (curve c). The recognition of HRP-Con A with poor electrical conductivity to the mannose on electrode surface also increased the electron-transfer resistance up to 3000 Ω (curve d), which showed the aggregates of proteins on the CNTs (Fig. S2c). These results demonstrated the immobilization of monose and the lectin recognition on the gate interface.

Optimization for biosensor preparation and mannose detection

The detection signal increased with the increasing amount of CNTs for biosensor preparation and reached the maximum value at the CNTs concentration of 1.0 mg/mL (Fig. S3a and S3b), indicating the full coverage of CNTs on gate interface for saturation binding of mannose via ADH. Thus, 10 μL of 1.0 mg/mL CNTs was used for preparation of CNT-modified gate electrode, at which the optimal concentration of mannose (10 μL) was selected as 2 μg/mL for the

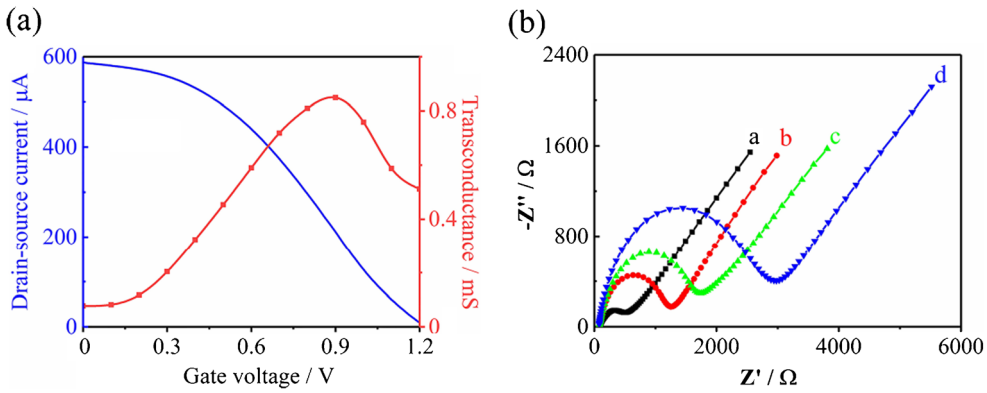

Fig. 2 (a) Transfer and transconductance curves of fresh OECT tested in PBS electrolyte. (b) EIS of a, CNTs; b, Man/ADH/CNTs; c, Man(BSA)/ADH/CNTs; and d, HRP-Con A-Man(BSA)/ADH/CNT-modified gate electrodes in 0.1 M KCl containing 5 mM $K_4[Fe(CN)_6]$/$K_3[Fe(CN)_6]$ (1:1). Frequency range: 100 kHz to 0.01 Hz; amplitude: 10 mV

preparation of OECT-based biosensor (Fig. S3c). After the modified gate interface was blocked with BSA, the detection signal increased with the increasing HRP-Con A concentration in the detection solution and trended to a steady value at 80 μg/mL due to the saturated recognition of the bound mannose (Fig. S3d). Thus, 80 μg/mL HRP-Con A was used for analysis of cell surface mannose.

Quantitative analysis of mannose on cell surface

To obtain the calibration curve of mannose, the mannose-modified gate electrodes were incubated with the mixtures of 80 μg/mL HRP-Con A and different concentrations of mannose, respectively. The normalized current response decreased with the increasing mannose concentration (Fig. 3a). The plot of the response versus the concentration of mannose showed a linearity with the equation of $\Delta I/I_0 = 0.542–0.254\ c_{Man}$ (Fig. 3b), and the limit of detection was calculated as 0.135 μg/mL (3σ/m). Besides, the change of effective gate voltage (ΔV_g^{eff}) of mannose sensor, which could be exacted from the transfer curve of device and the current response, also showed linear decrease with the increasing mannose concentration (Fig. S4). Since the detected device was the same as that for competitive analysis of cell surface glycan, these relationships could be used as the calibration curves for mannose analysis on cell surface.

For mannose analysis on cell surface, the mixture of 80 μg/mL HRP-Con A and different amounts of HeLa cells was incubated on mannose-modified gate interface. After competitive recognition, the current response decreased with the increasing amounts of cells (Fig. 3c). The plot of detection signal versus the cell number also showed a linearity with the equation of $\Delta I/I_0 = 0.501–2.60 \times 10^{-6}\ N_{cell}$ (Fig. 3d). From the plot and the calibration curve, the amount of mannose expressed on each HeLa cell was calculated to be 3.41×10^8, which was close to the values reported previously [28–31].

The recognition selectivity of lectin to mannose was evaluated with several monoses (Fig. S5). The mannose sensor showed negligible response to galactose, glucose, lactose, and sucrose, confirming the excellent specificity of the designed sensor.

Quantitative analysis of galactose on cell surface

The galactose-modified gate interface and HRP-PNA were used to realize the quantitative analysis of cell surface galactose. The optimal concentration of galactose for biosensor preparation was also 2.0 μg/mL (Fig. S6a). Similarly, 80 μg/mL HRP-PNA was used for full recognition of the immobilized galactose (Fig. S6b). The channel current response decreased with the increasing galactose concentration in incubation solution (Fig. S7a). The plots of both the channel

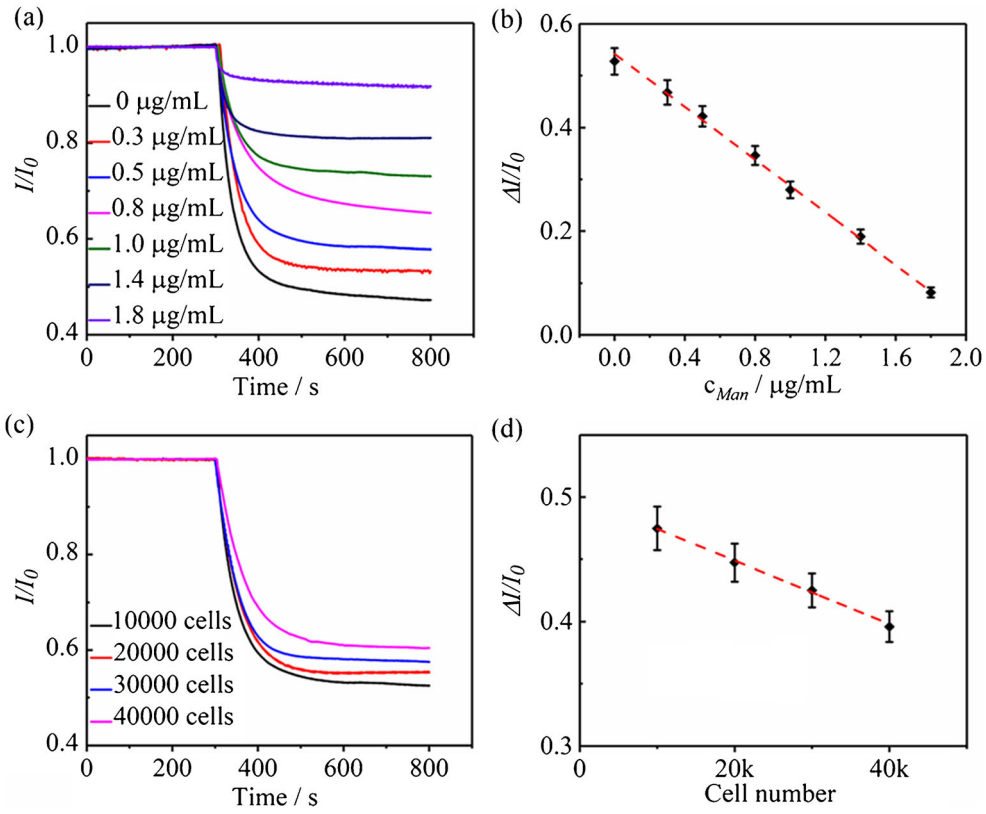

Fig. 3 Normalized current response of mannose sensor in pH 7.4 PBS containing 100 μM H_2O_2 to (a) mannose and (c) cells used for competitive recognition to 80 μg/mL HRP-Con A with 1-h incubation. Plot of (b) $\Delta I/I_0$ versus mannose concentration and (d) $\Delta I/I_0$ versus cell number. The drain-source voltage and gate voltage were fixed at 0.05 V and 0.9 V, respectively.

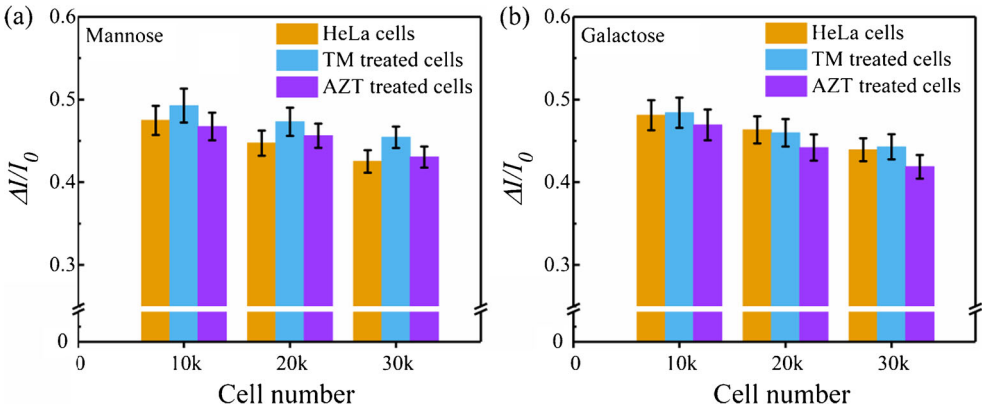

Fig. 4. $\Delta I/I_0$ values of mannose (a) and galactose (b) sensors after competitive recognition to 80 μg/mL HRP-Con A (a) or HRP-PNA (b) with different numbers of cells or TM and AZT-treated cells. The drain-source voltage and gate voltage were fixed at 0.05 V and 0.9 V, respectively.

current response and ΔV_g^{eff} versus the concentration of galactose (Fig. S7b and S8) could be used as the calibration curves for galactose analysis on cell surface. The detection limit was calculated as 0.159 μg/mL (3σ/m). This biosensor showed high selectivity towards galactose detection (Fig. S9). As another proof-of-concept, the HeLa cells were detected with the galactose biosensor (Fig. S7c and S7d), which showed the galactose amount of 2.92×10^8 expressed on each HeLa cell.

Expression changes of glycans on cell surface

The changes of glycan expressions on cell surface upon TM or AZT treatment were detected with the proposed OECT-based biosensors. After HeLa cells were cultured with 0.2 μM TM for 24 h, different amounts of cells were mixed with HRP-Con A or HRP-PNA to competitively recognize mannose or galactose immobilized sensor surfaces. As shown in Fig. 4, the TM treatment led to obvious increase of detection signal for mannose analysis on cell surface, while the signal for galactose analysis on cell surface did not show significant change (Fig. 4a), indicating that the TM inhibited the mannose expression, but did not affect the galactose expression on HeLa surface. On the contrary, the mannose expression did not change, and the galactose expression increased upon the AZT treatment (Fig. 4b). The results demonstrated that the expressions of mannose and galactose were sensitive to TM and AZT, respectively, which were consistent with the reported results [32–34]. These results were also confirmed by the flow cytometric analysis (Fig. S10), showing the potential application of the proposed strategy for glycan analysis on cell surface.

Application of OECT-based biosensors for analysis of serum samples

The proposed OECT-based biosensor could also be used for analysis of serum samples. The mannose level in human serum samples is generally in the range of 50 to 100 μM [35]. After five-times diluting the serum samples with PBS for competitive recognition, the detection results with the proposed mannose and galactose sensors are listed in Table S1. In comparison with commercial ELISA kit, the OECT-based mannose sensor showed the relative errors ranging from 2.94 to 3.64%. The galactose analysis demonstrated the recovery from 97.3 to 104.6%. Thus, the proposed OECT-based biosensor also possessed excellent reliability and accuracy in serum sample analysis, indicating its more extensive application compared to other methods developed previously (Table S2).

Conclusion

This work proposes monose-modified OECTs for quantitative biosensing of glycan expressions on cell surface with a competitive strategy. This strategy can obtain the calibration curves with the monose standard solutions, thus greatly simplifies the quantitative detection of cell surface glycans. By using different HRP-lectins to competitively recognize corresponding glycans on cell surface and monoses on gate electrode interface for obtaining the detectable signals in the presence of H_2O_2, the quantitation of both mannose and galactose expressions on HeLa cell surface has successfully been achieved. The designed biosensors can be used to monitor the changes of glycan expressions on cell surface upon different treatments. This work extends the convenient application of OECTs in cell surface glycan analysis and cytosensing.

Supplementary Information The online version contains supplementary material available at https://doi.org/10.1007/s00604-021-04918-7.

Funding This work was supported by the National Natural Science Foundation of China (21361162002, 21635005, 21827812, 21890741) and the program B for outstanding Ph.D. candidate of Nanjing University.

Declarations

Conflict of interest The authors declare no competing interests.

References

1. Mariño K, Bones J, Kattla JJ, Rudd PM (2010) A systematic approach to protein glycosylation analysis: a path through the maze. Nat Chem Biol 6:713–723. https://doi.org/10.1038/nchembio.437
2. Krasnova L, Wong C (2016) Understanding the chemistry and biology of glycosylation with glycan synthesis. Annu Rev Biochem 85:599–630. https://doi.org/10.1146/annurev-biochem-060614-034420
3. Chen YL, Ding L, Ju HX (2018) In situ cellular glycan analysis. Acc Chem Res 51(4):890–899. https://doi.org/10.1021/acs.accounts.7b00617
4. Krishnamoorthy L, Mahal LK (2009) Glycomic analysis: an array of technologies. ACS Chem. Biol 4(9):715–732. https://doi.org/10.1021/cb900103n
5. Lau KS, Dennis JW (2008) N-glycans in cancer progression. Glycobiology 18(10):750–760. https://doi.org/10.1093/glycob/cwn071
6. Xiao H, Wood EC, Vukojicic P, Bertozzi CR (2016) Precision glycocalyx editing as a strategy for cancer immunotherapy. Proc Natl Acad Sci U S A 113(37):10304–10309. https://doi.org/10.1073/pnas.1608069113
7. Fuster MM, Esko JD (2007) The sweet and sour of cancer: glycans as novel therapeutic targets. Nat Rev Cancer 5:526–542. https://doi.org/10.1038/nrc1649
8. Chen YL, Ding L, Xu JQ, Song WY, Yang M, Hu JJ, Ju HX (2015) Micro-competition system for Raman quantification of multiple glycans on intact cell surface. Chem Sci 6(7):3769–3774. https://doi.org/10.1039/c5sc01031d
9. Peng Y, Wang LM, Zhang Y, Bao HM, Lu HJ (2019) Stable isotope sequential derivatization for linkage-specific analysis of sialylated N-glycan isomers by MS. Anal Chem 91(24):15993–16001. https://doi.org/10.1021/acs.analchem.9b04727
10. Hamouda H, Kaup M, Ullah M, Berger M, Sandig V, Tauber R, Blanchard V (2014) Rapid analysis of cell surface N-glycosylation from living cells using mass spectrometry. J Proteome Res 13(12):6144–6151. https://doi.org/10.1021/pr5003005
11. Chen YL, Ding L, Liu TT, Ju HX (2013) Arrayed profiling of multiple glycans on whole living cell surfaces. Anal Chem 85(22):11153–11158. https://doi.org/10.1021/ac403150n
12. Cheng W, Ding L, Ding SJ, Yin YB, Ju HX (2009) A simple electrochemical cytosensor array for dynamic analysis of carcinoma cell surface glycans. Angew Chem Int Ed 48(35):6465–6468. https://doi.org/10.1002/anie.200902356
13. Han E, Ding L, Jin S, Ju HX (2011) Electrochemiluminescent biosensing of carbohydrate-functionalized CdS nanocomposites for in situ label-free analysis of cell surface carbohydrate. Biosens Bioelectron 26(5):2500–2505. https://doi.org/10.1016/j.bios.2010.10.044
14. Feng KJ, Liao FL, Yang MH (2020) Analysis of glycan expression on cell surfaces by using a glassy carbon electrode modified with MnO_2 nanosheets and DNA-generated electrochemical current. Microchim Acta 187:148. https://doi.org/10.1007/s00604-019-4084-3
15. Wang NX, Yang AN, Fu Y, Li YZ, Yan F (2019) Functionalized organic thin film transistors for biosensing. Acc Chem Res 52(2):277–287. https://doi.org/10.1021/acs.accounts.8b00448
16. Liao CZ, Zhang M, Yao MY, Hua T, Li L, Yan F (2015) Flexible organic electronics in biology: materials and devices. Adv Mater 27(46):7493–7527. https://doi.org/10.1002/adma.201402625
17. Rivnay J, Inal S, Salleo A, Owens RM, Berggren M, Malliaras GG (2018) Organic electrochemical transistors. Nat Rev Mater 3:17086. https://doi.org/10.1038/natrevmats.2017.86
18. Yang AN, Li YZ, Yang CX, Fu Y, Wang NX, Li L, Yan F (2018) Fabric organic electrochemical transistors for biosensors. Adv Mater 30(23):1800051. https://doi.org/10.1002/adma.201800051
19. Braendlein M, Pappa A, Ferro M, Lopresti A, Acquaviva C, Mamessier E, Malliaras GG, Owens RM (2017) Lactate detection in tumor cell cultures using organic transistor circuits. Adv Mater 29(13):1605744. https://doi.org/10.1002/adma.201605744
20. Diacci C, Lee JW, Janson P, Dufil G, Méhes G, Berggren M, Simon DT, Stavrinidou E (2020) Real-time monitoring of glucose export from isolated chloroplasts using an organic electrochemical transistor. Adv Mater Technol 5(3):1900262. https://doi.org/10.1002/admt.201900262
21. Guo X, Cao QQ, Liu YW, He T, Liu JW, Huang S, Tang H, Ma M (2020) Organic electrochemical transistor for in situ detection of H_2O_2 released from adherent cells and its application in evaluating the in vitro cytotoxicity of nanomaterial. Anal Chem 92(1):908–915. https://doi.org/10.1021/acs.analchem.9b03718
22. Wustoni S, Wang SF, Alvarez JR, Hidalgo TC, Nunes SP, Inal S (2019) An organic electrochemical transistor integrated with a molecularly selective isoporous membrane for amyloid-β detection. Biosens Bioelectron 143:111561. https://doi.org/10.1016/j.bios.2019.111561
23. Fu Y, Wang NX, Yang AN, Law HKW, Li L, Yan F (2017) Highly sensitive detection of protein biomarkers with organic electrochemical transistors. Adv Mater 29(41):1703787. https://doi.org/10.1002/adma.201703787
24. Parlak O, Keene S, Marais A, Curto V, Salleo A (2018) Molecularly selective nanoporous membrane-based wearable organic electrochemical device for noninvasive cortisol sensing. Sci Adv 4(7):eaar2904. https://doi.org/10.1126/sciadv.aar2904
25. He RX, Zhang M, Tan F, Leung PHM, Zhao XZ, Chan HLW, Yang M, Yan F (2012) Detection of bacteria with organic electrochemical transistors. J Mater Chem 22(41):22072–22076. https://doi.org/10.1039/c2jm33667g
26. Yu J, Yang AN, Wang NX, Ling HF, Song JJ, Chen X, Lian YD, Zhang ZS, Yan F, Gu M (2021) Highly sensitive detection of caspase-3 activity based on peptide-modified organic electrochemical transistor biosensors. Nanoscale 13(5):2868–2874. https://doi.org/10.1039/d0nr08453k
27. Chen LZ, Fu Y, Wang NX, Yang AN, Li YZ, Wu J, Ju HX, Yan F (2018) Organic electrochemical transistors for the detection of cell surface glycans. ACS Appl Mater Interfaces 10(22):18470–18477. https://doi.org/10.1021/acsami.8b01987
28. Chen LZ, Wu J, Yan F, Ju HX (2021) A facile strategy for quantitative sensing of glycans on cell surface using organic electrochemical transistors. Biosens Bioelectron 175:112878. https://doi.org/10.1016/j.bios.2020.112878
29. Ding L, Cheng W, Wang XJ, Ding SJ, Ju HX (2008) Carbohydrate monolayer strategy for electrochemical assay of cell surface carbohydrate. J Am Chem Soc 130(23):7224–7225. https://doi.org/10.1021/ja801468b
30. Xue YD, Ding L, Lei JP, Ju HX (2010) A simple electrochemical lectin-probe for in situ homogeneous cytosensing and facile evaluation of cell surface glycan. Biosens Bioelectron 26(1):169–174. https://doi.org/10.1016/j.bios.2010.06.010
31. Zhang XA, Teng YQ, Fu Y, Zhang SP, Wang T, Wang CG, Jin LT, Zhang W (2011) Lectin-based electrochemical biosensor constructed by functionalized carbon nanotubes for the competitive assay of glycan expression on living cancer cells. Chem Sci 2(12):2353–2360. https://doi.org/10.1039/c1sc00562f
32. Helenius A, Aebi M (2001) Intracellular functions of N-linked glycans. Science 291(5512):2364–2369. https://doi.org/10.1126/science.291.5512.2364
33. Chen XJ, Wang YZ, Zhang YY, Chen ZH, Liu Y, Li ZL, Li JH (2014) Sensitive electrochemical aptamer biosensor for dynamic cell surface N-glycan evaluation featuring multivalent recognition

and signal amplification on a dendrimer-graphene electrode interface. Anal Chem 86(9):4278–4286. https://doi.org/10.1021/ac404070m

34. Steet RA, Melancon P, Kuchta RD (2000) 3′-Azidothymidine potently inhibits the biosynthesis of highly branched N-linked oligosaccharides and poly-N-acetyllactosamine chains in cells. J Biol Chem 275(35):26812–26820. https://doi.org/10.1074/jbc.m004038200
35. Yoshimura K, Hirano S, Takata H, Funakoshi S, Ohmi S, Amano E, Nishi Y, Inoue M, Fukuda Y, Hayashi H, Taguchi T, Yamada S, Miwa I, Terada Y, Shimpei Fujimoto S (2017) Plasma mannose level, a putative indicator of glycogenolysis, and glucose tolerance in Japanese individuals. J Diabetes Investig 8(4):489–495. https://doi.org/10.1111/jdi.12622